

Search for New Color-Octet Vector Particle Decaying to
 $t\bar{t}$ in $p\bar{p}$ Collisions at $\sqrt{s} = 1.96$ TeV

T. Aaltonen^x, J. Adelmanⁿ, B. Álvarez González^{l,1}, S. Amerio^{ar}, D. Amidei^{ai},
A. Anastasov^{am}, A. Annovi^t, J. Antos^o, G. Apollinari^r, A. Apresyan^{aw},
T. Arisawa^{bf}, A. Artikov^p, J. Asaadi^{bb}, W. Ashmanskas^r, A. Attal^d,
A. Aurisano^{bb}, F. Azfar^{aq}, W. Badgett^r, A. Barbaro-Galtieri^{ac}, V.E. Barnes^{aw},
B.A. Barnett^z, P. Barria^{au}, P. Bartos^o, G. Bauer^{ag}, P.-H. Beauchemin^{ah},
F. Bedeschi^{au}, D. Beecher^{ae}, S. Behari^z, G. Bellettini^{au}, J. Bellinger^{bh},
D. Benjamin^q, A. Beretvas^r, A. Bhatti^{ay}, M. Binkley^r, D. Bisello^{ar},
I. Bizjak^{ae,1}, R.E. Blair^b, C. Blocker^g, B. Blumenfeld^z, A. Bocchi^q, A. Bodek^{ax},
V. Boisvert^{ax}, D. Bortoletto^{aw}, J. Boudreau^{av}, A. Boveia^k, B. Brau^{k,1},
A. Bridgeman^y, L. Brigliadori^f, C. Bromberg^{aj}, E. Brubakerⁿ, J. Budagov^p,
H.S. Budd^{ax}, S. Budd^y, K. Burkett^f, G. Busetto^{ar}, P. Bussey^v, A. Buzatu^{ah},
K. L. Byrum^b, S. Cabrera^{q,1}, C. Calancha^{af}, S. Camarda^d, M. Campanelli^{ae},
M. Campbell^{ai}, F. Canelli^{n,r}, A. Canepa^{at}, B. Carls^y, D. Carlsmith^{bh},
R. Carosi^{au}, S. Carrillo^{s,1}, S. Carron^r, B. Casal^l, M. Casarsa^r, A. Castro^f,
P. Catastini^{au}, D. Cauz^{bc}, V. Cavaliere^{au}, M. Cavalli-Sforza^d, A. Cerri^{ac},
L. Cerrito^{ae,1}, S.H. Chang^{ab}, Y.C. Chen^a, M. Chertok^h, G. Chiarelli^{au},
G. Chlachidze^r, F. Chlebana^r, K. Cho^{ab}, D. Chokheli^p, J.P. Chou^w,
K. Chung^{r,1}, W.H. Chung^{bh}, Y.S. Chung^{ax}, T. Chwalek^{aa}, C.I. Ciobanu^{as},
M.A. Ciocci^{au}, A. Clark^u, D. Clark^g, G. Compostella^{ar}, M.E. Convery^r,
J. Conway^h, M. Corbo^{as}, M. Cordelli^t, C.A. Cox^h, D.J. Cox^h, F. Crescioli^{au},
C. Cuenca Almenar^{bi}, J. Cuevas^{l,1}, R. Culbertson^r, J.C. Cully^{ai},
D. Dagenhart^r, M. Datta^r, T. Davies^v, P. de Barbaro^{ax}, S. De Cecco^{az},
A. Deisher^{ac}, G. De Lorenzo^d, M. Dell'Orso^{au}, C. Deluca^d, L. Demortier^{ay},
J. Deng^{q,1}, M. Deninno^f, M. d'Errico^{ar}, A. Di Canto^{au}, G.P. di Giovanni^{as},
B. Di Ruzza^{au}, J.R. Dittmann^e, M. D'Onofrio^d, S. Donati^{au}, P. Dong^r,
T. Dorigo^{ar}, S. Dube^{ba}, K. Ebina^{bf}, A. Elagin^{bb}, R. Erbacher^h, D. Errede^y,
S. Errede^y, N. Ershaidat^{as,1}, R. Eusebi^{bb}, H.C. Fang^{ac}, S. Farrington^{aq},
W.T. Fedorkoⁿ, R.G. Feild^{bi}, M. Feindt^{aa}, J.P. Fernandez^{af}, C. Ferrazza^{au},
R. Field^s, G. Flanagan^{aw,1}, R. Forrest^h, M.J. Frank^e, M. Franklin^w,
J.C. Freeman^r, I. Furic^s, M. Gallinaro^{ay}, J. Galyardt^m, F. Garberon^k,
J.E. Garcia^u, A.F. Garfinkel^{aw}, P. Garosi^{au}, H. Gerberich^y, D. Gerdes^{ai},
A. Gessler^{aa}, S. Giagu^{az}, V. Giakoumopoulou^c, P. Giannetti^{au}, K. Gibson^{av},
J.L. Gimmell^{ax}, C.M. Ginsburg^r, N. Giokaris^c, M. Giordani^{bc}, P. Giromini^t,
M. Giunta^{au}, G. Giurgiu^z, V. Glagolev^p, D. Glenzinski^r, M. Gold^{al},
N. Goldschmidt^s, A. Golossanov^r, G. Gomez^l, G. Gomez-Ceballos^{ag},
M. Goncharov^{ag}, O. González^{af}, I. Gorelov^{al}, A.T. Goshaw^q, K. Goulios^{ay},
A. Greife^{ar}, S. Grinstein^d, C. Grosso-Pilcherⁿ, R.C. Group^r, U. Grundler^y,
J. Guimaraes da Costa^w, Z. Gunay-Unalan^{aj}, C. Haber^{ac}, S.R. Hahn^r,
E. Halkiadakis^{ba}, B.-Y. Han^{ax}, J.Y. Han^{ax}, F. Happacher^t, K. Hara^{bd},
D. Hare^{ba}, M. Hare^{be}, R.F. Harr^{bg}, M. Hartz^{av}, K. Hatakeyama^e, C. Hays^{aq},
M. Heck^{aa}, J. Heinrich^{at}, M. Herndon^{bh}, J. Heuser^{aa}, S. Hewamanage^e,

D. Hidas^{ba}, C.S. Hill^{k,1}, D. Hirschbuehl^{aa}, A. Hocker^r, S. Hou^a, M. Houlden^{ad},
 S.-C. Hsu^{ac}, R.E. Hughes^{an}, M. Hurwitzⁿ, U. Husemann^{bi}, M. Hussein^{aj},
 J. Huston^{aj}, J. Incandela^k, G. Introzzi^{au}, M. Iori^{az}, A. Ivanov^{h,1}, E. James^r,
 D. Jang^m, B. Jayatilaka^q, E.J. Jeon^{ab}, M.K. Jha^f, S. Jindariani^r,
 W. Johnson^h, M. Jones^{aw}, K.K. Joo^{ab}, S.Y. Jun^m, J.E. Jung^{ab}, T.R. Junk^r,
 T. Kamon^{bb}, D. Kar^s, P.E. Karchin^{bg}, Y. Kato^{ap,1}, R. Kephart^r,
 W. Ketchumⁿ, J. Keung^{at}, V. Khotilovich^{bb}, B. Kilminster^r, D.H. Kim^{ab},
 H.S. Kim^{ab}, H.W. Kim^{ab}, J.E. Kim^{ab}, M.J. Kim^t, S.B. Kim^{ab}, S.H. Kim^{bd},
 Y.K. Kimⁿ, N. Kimura^{bf}, L. Kirsch^g, S. Klimentenko^s, K. Kondo^{bf}, D.J. Kong^{ab},
 J. Konigsberg^s, A. Korytov^s, A.V. Kotwal^q, M. Kreps^{aa}, J. Kroll^{at}, D. Kropⁿ,
 N. Krumnack^e, M. Kruse^q, V. Krutelyov^k, T. Kuhr^{aa}, N.P. Kulkarni^{bg},
 M. Kurata^{bd}, S. Kwangⁿ, A.T. Laasanen^{aw}, S. Lami^{au}, S. Lammell^r,
 M. Lancaster^{ae}, R.L. Lander^h, K. Lannon^{an,1}, A. Lath^{ba}, G. Latino^{au},
 I. Lazzizzera^{ar}, T. LeCompte^b, E. Lee^{bb}, H.S. Leeⁿ, J.S. Lee^{ab}, S.W. Lee^{bb,1},
 S. Leone^{au}, J.D. Lewis^r, C.-J. Lin^{ac}, J. Linacre^{aq}, M. Lindgren^r, E. Lipeles^{at},
 A. Lister^u, D.O. Litvintsev^r, C. Liu^{av}, T. Liu^r, N.S. Lockyer^{at}, A. Loginov^{bi},
 L. Lovas^o, D. Lucchesi^{ar}, J. Lueck^{aa}, P. Lujan^{ac}, P. Lukens^r, G. Lungu^{ay},
 J. Lys^{ac}, R. Lysak^o, D. MacQueen^{ah}, R. Madrak^r, K. Maeshima^f,
 K. Makhoul^{ag}, P. Maksimovic^z, S. Malde^{aq}, S. Malik^{ae}, G. Manca^{ad,1},
 A. Manousakis-Katsikakis^c, F. Margaroli^{aw}, C. Marino^{aa}, C.P. Marino^y,
 A. Martin^{bi}, V. Martin^{v,1}, M. Martínez^d, R. Martínez-Ballarín^{af},
 P. Mastrandrea^{az}, M. Mathis^z, M.E. Mattson^{bg}, P. Mazzanti^f,
 K.S. McFarland^{ax}, P. McIntyre^{bb}, R. McNulty^{ad,1}, A. Mehta^{ad}, P. Mehtala^x,
 A. Menzione^{au}, C. Mesropian^{ay}, T. Miao^f, D. Mietlicki^{ai}, N. Miladinovic^g,
 R. Miller^{aj}, C. Mills^w, M. Milnik^{aa}, A. Mitra^a, G. Mitselmakher^s, H. Miyake^{bd},
 S. Moed^w, N. Moggi^f, M.N. Mondragon^{r,1}, C.S. Moon^{ab}, R. Moore^r,
 M.J. Morello^{au}, J. Morlock^{aa}, P. Movilla Fernandez^r, J. Mülmenstädt^{ac},
 A. Mukherjee^r, Th. Muller^{aa}, P. Murat^r, M. Mussini^f, J. Nachtman^{r,1},
 Y. Nagai^{bd}, J. Naganoma^{bd}, K. Nakamura^{bd}, I. Nakano^{ao}, A. Napier^{be},
 J. Nett^{bh}, C. Neu^{at,1}, M.S. Neubauer^y, S. Neubauer^{aa}, J. Nielsen^{ac,1},
 L. Nodulman^b, M. Norman^j, O. Norniella^y, E. Nurse^{ae}, L. Oakes^{aq}, S.H. Oh^q,
 Y.D. Oh^{ab}, I. Oksuzian^s, T. Okusawa^{ap}, R. Orava^x, K. Osterberg^x,
 S. Pagan Griso^{ar}, C. Pagliarone^{bc}, E. Palencia^r, V. Papadimitriou^r,
 A. Papaikonomou^{aa}, A.A. Paramanov^b, B. Parks^{an}, S. Pashapour^{ah},
 J. Patrick^r, G. Pauletta^{bc}, M. Paulini^m, C. Paus^{ag}, T. Peiffer^{aa}, D.E. Pellett^h,
 A. Penzo^{bc}, T.J. Phillips^q, G. Piacentino^{au}, E. Pianori^{at}, L. Pinera^s, K. Pitts^y,
 C. Plagerⁱ, L. Pondrom^{bh}, K. Potamianos^{aw}, O. Poukhov^{p,1}, F. Prokoshin^{p,1},
 A. Pronko^r, F. Ptohos^{r,1}, E. Pueschel^m, G. Punzi^{au}, J. Pursley^{bh},
 J. Rademacker^{aq,1}, A. Rahaman^{av}, V. Ramakrishnan^{bh}, N. Ranjan^{aw},
 I. Redondo^{af}, P. Renton^{aq}, M. Renz^{aa}, M. Rescigno^{az}, S. Richter^{aa},
 F. Rimondi^f, L. Ristori^{au}, A. Robson^v, T. Rodrigo^l, T. Rodriguez^{at},
 E. Rogers^y, S. Rolli^{be}, R. Roser^r, M. Rossi^{bc}, R. Rossin^k, P. Roy^{ah}, A. Ruiz^l,
 J. Russ^m, V. Rusu^r, B. Rutherford^r, H. Saarikko^x, A. Safonov^{bb},
 W.K. Sakamoto^{ax}, L. Santi^{bc}, L. Sartori^{au}, K. Sato^{bd}, A. Savoy-Navarro^{as},
 P. Schlabach^r, A. Schmidt^{aa}, E.E. Schmidt^r, M.A. Schmidtⁿ, M.P. Schmidt^{bi},
 M. Schmitt^{am}, T. Schwarz^h, L. Scodellaro^l, A. Scribano^{au}, F. Scuri^{au},

A. Sedov^{aw}, S. Seidel^{al}, Y. Seiya^{ap}, A. Semenov^p, L. Sexton-Kennedy^r,
 F. Sforza^{au}, A. Sfyrla^y, S.Z. Shalhout^{bg}, T. Shears^{ad}, P.F. Shepard^{av},
 M. Shimojima^{bd,1}, S. Shiraishiⁿ, M. Shochetⁿ, Y. Shon^{bh}, I. Shreyber^{ak},
 A. Simonenko^p, P. Sinervo^{ah}, A. Sisakyan^p, A.J. Slaughter^r, J. Slaunwhite^{an},
 K. Sliwa^{be}, J.R. Smith^h, F.D. Snider^r, R. Snihur^{ah}, A. Soha^r, S. Somalwar^{ba},
 V. Sorin^d, P. Squillacioti^{au}, M. Stanitzki^{bi}, R. St. Denis^v, B. Stelzer^{ah},
 O. Stelzer-Chilton^{ah}, D. Stentz^{am}, J. Strologas^{al}, G.L. Strycker^{ai}, J.S. Suh^{ab},
 A. Sukhanov^s, I. Suslov^p, A. Taffard^{y,1}, R. Takashima^{ao}, Y. Takeuchi^{bd},
 R. Tanaka^{ao}, J. Tangⁿ, M. Tecchio^{ai}, P.K. Teng^a, J. Thom^{r,1}, J. Thome^m,
 G.A. Thompson^y, E. Thomson^{at}, P. Tipton^{bi}, P. Ttito-Guzmán^{af}, S. Tkaczyk^r,
 D. Toback^{bb}, S. Tokar^o, K. Tollefson^{aj}, T. Tomura^{bd}, D. Tonelli^r, S. Torre^t,
 D. Torretta^r, P. Totaro^{bc}, S. Tournear^{as}, M. Trovato^{au}, S.-Y. Tsai^a, Y. Tu^{at},
 N. Turini^{au}, F. Ukegawa^{bd}, S. Uozumi^{ab}, N. van Remortel^{x,1}, A. Varganov^{ai},
 E. Vataga^{au}, F. Vázquez^{s,1}, G. Velev^r, C. Vellidis^c, M. Vidal^{af}, I. Vila^l,
 R. Vilar^l, M. Vogel^{al}, I. Volobouev^{ac,1}, G. Volpi^{au}, P. Wagner^{at}, R.G. Wagner^b,
 R.L. Wagner^r, W. Wagner^{aa,1}, J. Wagner-Kuhr^{aa}, T. Wakisaka^{ap}, R. Wallnyⁱ,
 S.M. Wang^a, A. Warburton^{ah}, D. Waters^{ae}, M. Weinberger^{bb}, J. Weinelt^{aa},
 W.C. Wester III^r, B. Whitehouse^{be}, D. Whiteson^{at,1}, A.B. Wicklund^b,
 E. Wicklund^r, S. Wilburⁿ, G. Williams^{ah}, H.H. Williams^{at}, P. Wilson^r,
 B.L. Winer^{an}, P. Wittich^{r,1}, S. Wolbers^r, C. Wolfeⁿ, H. Wolfe^{an}, T. Wright^{ai},
 X. Wu^u, F. Würthwein^j, A. Yagil^j, K. Yamamoto^{ap}, J. Yamaoka^q,
 U.K. Yang^{n,1}, Y.C. Yang^{ab}, W.M. Yao^{ac}, G.P. Yeh^r, K. Yi^{r,1}, J. Yoh^r,
 K. Yorita^{bf}, T. Yoshida^{ap,1}, G.B. Yu^q, I. Yu^{ab}, S.S. Yu^r, J.C. Yun^r,
 A. Zanetti^{bc}, Y. Zeng^q, X. Zhang^y, Y. Zheng^{i,1}, S. Zucchelli^f,

(CDF Collaboration *)

¹Visitor from University de Oviedo, E-33007 Oviedo, Spain. ²On leave from J. Stefan Institute, Ljubljana, Slovenia. ³Visitor from University of Massachusetts Amherst, Amherst, Massachusetts 01003, United States. ⁴Visitor from IFIC(CSIC-Universitat de Valencia), 56071 Valencia, Spain. ⁵Visitor from Universidad Iberoamericana, Mexico D.F., Mexico. ⁶Visitor from Queen Mary, University of London, London, E1 4NS, England. ⁷Visitor from University of Iowa, Iowa City, IA 52242, United States. ⁸Visitor from University of California Irvine, Irvine, CA 92697, United States. ⁹Visitor from Yarmouk University, Irbid 211-63, Jordan. ¹⁰Visitor from Muons, Inc., Batavia, IL 60510, United States. ¹¹Visitor from University of Bristol, Bristol BS8 1TL, United Kingdom. ¹²Visitor from Kansas State University, Manhattan, KS 66506, United States. ¹³Visitor from Kinki University, Higashi-Osaka City 577-8502, Japan. ¹⁴Visitor from University of Notre Dame, Notre Dame, IN 46556, United States. ¹⁵Visitor from Texas Tech University, Lubbock, TX 79609, United States. ¹⁶Visitor from Istituto Nazionale di Fisica Nucleare, Sezione di Cagliari, 09042 Monserrato (Cagliari), Italy. ¹⁷Visitor from University of Edinburgh, Edinburgh EH9 3JZ, United Kingdom. ¹⁸Visitor from University College Dublin, Dublin 4, Ireland. ¹⁹Visitor from University of Virginia, Charlottesville, VA 22906, United States. ²⁰Visitor from University of California Santa Cruz, Santa Cruz, CA 95064, United States. ²¹Deceased. ²²Visitor from Universidad Tecnica Federico Santa Maria, 110v Valparaiso, Chile. ²³Visitor from University of Cyprus, Nicosia CY-1678, Cyprus. ²⁴Visitor from Nagasaki Institute of Applied Science, Nagasaki, Japan. ²⁵Visitor from Cornell University, Ithaca, NY 14853, United States. ²⁶Visitor from Universiteit Antwerpen, B-2610 Antwerp, Belgium. ²⁷Visitor from Bergische Universität Wuppertal, 42097 Wuppertal, Germany. ²⁸Visitor from University of Manchester, Manchester M13 9PL, England. ²⁹Visitor from University of Fukui, Fukui City, Fukui Prefecture 910-0017, Japan.

- ^a*Institute of Physics, Academia Sinica, Taipei, Taiwan 11529, Republic of China*
- ^b*Argonne National Laboratory, Argonne, Illinois 60439, United States*
- ^c*University of Athens, 157 71 Athens, Greece*
- ^d*Institut de Física d'Altes Energies, Universitat Autònoma de Barcelona, E-08193, Bellaterra (Barcelona), Spain*
- ^e*Baylor University, Waco, Texas 76798, United States*
- ^f*Istituto Nazionale di Fisica Nucleare Bologna, University of Bologna, I-40127 Bologna, Italy*
- ^g*Brandeis University, Waltham, Massachusetts 02254, United States*
- ^h*University of California, Davis, Davis, California 95616, United States*
- ⁱ*University of California, Los Angeles, Los Angeles, California 90024, United States*
- ^j*University of California, San Diego, La Jolla, California 92093, United States*
- ^k*University of California, Santa Barbara, Santa Barbara, California 93106, United States*
- ^l*Instituto de Física de Cantabria, CSIC-University of Cantabria, 39005 Santander, Spain*
- ^m*Carnegie Mellon University, Pittsburgh, PA 15213, United States*
- ⁿ*Enrico Fermi Institute, University of Chicago, Chicago, Illinois 60637, United States*
- ^o*Comenius University, 842 48 Bratislava, Slovakia; Institute of Experimental Physics, 040 01 Kosice, Slovakia*
- ^p*Joint Institute for Nuclear Research, RU-141980 Dubna, Russia*
- ^q*Duke University, Durham, North Carolina 27708, United States*
- ^r*Fermi National Accelerator Laboratory, Batavia, Illinois 60510, United States*
- ^s*University of Florida, Gainesville, Florida 32611, United States*
- ^t*Laboratori Nazionali di Frascati, Istituto Nazionale di Fisica Nucleare, I-00044 Frascati, Italy*
- ^u*University of Geneva, CH-1211 Geneva 4, Switzerland*
- ^v*Glasgow University, Glasgow G12 8QQ, United Kingdom*
- ^w*Harvard University, Cambridge, Massachusetts 02138, United States*
- ^x*Division of High Energy Physics, Department of Physics, University of Helsinki and Helsinki Institute of Physics, FIN-00014, Helsinki, Finland*
- ^y*University of Illinois, Urbana, Illinois 61801, United States*
- ^z*The Johns Hopkins University, Baltimore, Maryland 21218, United States*
- ^{aa}*Institut für Experimentelle Kernphysik, Karlsruhe Institute of Technology, D-76131 Karlsruhe, Germany*
- ^{ab}*Center for High Energy Physics: Kyungpook National University, Daegu 702-701, Korea; Seoul National University, Seoul 151-742, Korea; Sungkyunkwan University, Suwon 440-746, Korea; Korea Institute of Science and Technology Information, Daejeon 305-806, Korea; Chonnam National University, Gwangju 500-757, Korea; Chonbuk National University, Jeonju 561-756, Korea*
- ^{ac}*Ernest Orlando Lawrence Berkeley National Laboratory, Berkeley, California 94720, United States*
- ^{ad}*University of Liverpool, Liverpool L69 7ZE, United Kingdom*
- ^{ae}*University College London, London WC1E 6BT, United Kingdom*
- ^{af}*Centro de Investigaciones Energeticas Medioambientales y Tecnológicas, E-28040 Madrid, Spain*
- ^{ag}*Massachusetts Institute of Technology, Cambridge, Massachusetts 02139, United States*
- ^{ah}*Institute of Particle Physics: McGill University, Montréal, Québec, H3A 2T8; Simon Fraser University, Burnaby, British Columbia, V5A 1S6; University of Toronto, Toronto, Ontario, M5S 1A7; and TRIUMF, Vancouver, British Columbia, V6T 2A3, Canada*
- ^{ai}*University of Michigan, Ann Arbor, Michigan 48109, United States*
- ^{aj}*Michigan State University, East Lansing, Michigan 48824, United States*
- ^{ak}*Institution for Theoretical and Experimental Physics, ITEP, Moscow 117259, Russia*
- ^{al}*University of New Mexico, Albuquerque, New Mexico 87131, United States*
- ^{am}*Northwestern University, Evanston, Illinois 60208, United States*
- ^{an}*The Ohio State University, Columbus, Ohio 43210, United States*

³⁰Visitor from Chinese Academy of Sciences, Beijing 100864, China.

- ^{ao}Okayama University, Okayama 700-8530, Japan
^{ap}Osaka City University, Osaka 588, Japan
^{aq}University of Oxford, Oxford OX1 3RH, United Kingdom
^{ar}Istituto Nazionale di Fisica Nucleare, Sezione di Padova-Trento, University of Padova,
I-35131 Padova, Italy
^{as}LPNHE, Universite Pierre et Marie Curie/IN2P3-CNRS, UMR7585, Paris, F-75252
France
^{at}University of Pennsylvania, Philadelphia, Pennsylvania 19104, United States
^{au}Istituto Nazionale di Fisica Nucleare Pisa, University of Pisa, University of Siena and
Scuola Normale Superiore, I-56127 Pisa, Italy
^{av}University of Pittsburgh, Pittsburgh, Pennsylvania 15260, United States
^{aw}Purdue University, West Lafayette, Indiana 47907, United States
^{ax}University of Rochester, Rochester, New York 14627, United States
^{ay}The Rockefeller University, New York, New York 10021, United States
^{az}Istituto Nazionale di Fisica Nucleare, Sezione di Roma 1, Sapienza Università di Roma,
I-00185 Roma, Italy
^{ba}Rutgers University, Piscataway, New Jersey 08855, United States
^{bb}Texas A&M University, College Station, Texas 77843, United States
^{bc}Istituto Nazionale di Fisica Nucleare Trieste/Udine, I-34100 Trieste, University of
Trieste/Udine, I-33100 Udine, Italy
^{bd}University of Tsukuba, Tsukuba, Ibaraki 305, Japan
^{be}Tufts University, Medford, Massachusetts 02155, United States
^{bf}Waseda University, Tokyo 169, Japan
^{bg}Wayne State University, Detroit, Michigan 48201, United States
^{bh}University of Wisconsin, Madison, Wisconsin 53706, United States
^{bi}Yale University, New Haven, Connecticut 06520, United States

Abstract

We present the result of a search for a massive color-octet vector particle, (e.g. a massive gluon) decaying to a pair of top quarks in proton-antiproton collisions with a center-of-mass energy of 1.96 TeV. This search is based on 1.9 fb^{-1} of data collected using the CDF detector during Run II of the Tevatron at Fermilab. We study $t\bar{t}$ events in the lepton+jets channel with at least one b -tagged jet. A massive gluon is characterized by its mass, decay width, and the strength of its coupling to quarks. These parameters are determined according to the observed invariant mass distribution of top quark pairs. We set limits on the massive gluon coupling strength for masses between 400 and 800 GeV/c^2 and width-to-mass ratios between 0.05 and 0.50. The coupling strength of the hypothetical massive gluon to quarks is consistent with zero within the explored parameter space.

Keywords: massive gluon, top quark

PACS: 13.85.Rm, 14.65.Ha, 14.80.-j

1. Introduction

The top quark is the heaviest known elementary particle, with a mass very close to the electroweak symmetry-breaking scale. As such, the top could be sensitive to physics beyond the standard model (SM) [1, 2]. New particles decaying to $t\bar{t}$ pairs can be scalar or vector, color-singlet or color-octet; a scalar resonance is predicted in two-Higgs-doublets models [3, 4]; vector particles appear as massive Z -like bosons in extended gauge theories [5], or as Kaluza-Klein states of the gluon and Z boson [6, 7], or as colorons [1]. Searches for a color-singlet particle decaying to a $t\bar{t}$ pair have been performed by CDF and D0 collaborations in Run I [8, 9] and Run II [10, 11, 12].

In this Letter we describe a search for a massive color-octet vector particle G , which we call generically a “massive gluon”. We assume G has a much stronger coupling to the top quark than to the lighter quarks, $q = (u, d, c, s, b)$ [1]. We also assume the massive-massless gluon coupling is negligible. A Feynman diagram for $t\bar{t}$ production via massive-gluon is shown in Fig. 1. The coupling strength of massive gluons to light and top quarks are $\lambda_q g_s$ and $\lambda_t g_s$, respectively, where g_s is the coupling constant of the SM strong interaction.

In $t\bar{t}$ production, there are three observable parameters: the product of massive gluon coupling strength $\lambda \equiv \lambda_q \lambda_t$, mass M , and width Γ . In this analysis we consider only the possibility of novel strong-sector production; we assume that the weak decay of the top quark follows the SM. Since the color and the current structures of G and SM gluon (g) are identical, interference between processes through massive gluon and massless gluon will produce a $t\bar{t}$ invariant mass distribution with an enhanced signal that has a characteristic form [1] as shown later in Fig. 3. If the coupling of G to quarks is assumed to be parity-conserving, the production matrix element can be written as

$$|\mathcal{M}_{\text{prod.}}|^2 = \frac{2}{9} g_s^4 \hat{s}^2 (2 - \beta^2 + \beta^2 \cos^2 \theta) (\Pi_g + \lambda \Pi_{\text{int.}} + \lambda^2 \Pi_G), \quad (1)$$

where \hat{s} , β , and θ are the $t\bar{t}$ invariant mass squared, the velocity of the top quark, and the angle between the top quark and the incident quark in the $t\bar{t}$ center of mass system, respectively. The propagator factors of gluons, massive gluons, and interference are

$$\Pi_g = \frac{1}{\hat{s}^2}, \quad \Pi_G = \frac{1}{(\hat{s} - M^2)^2 + M^2 \Gamma^2}, \quad \Pi_{\text{int.}} = \frac{2}{\hat{s}} \frac{\hat{s} - M^2}{(\hat{s} - M^2)^2 + M^2 \Gamma^2}. \quad (2)$$

We search for $t\bar{t}$ pairs produced by massive and massless gluons, where interference between these diagrams (denoted by $g + G$) is considered, by examining the invariant mass spectrum of observed $t\bar{t}$ candidate events.

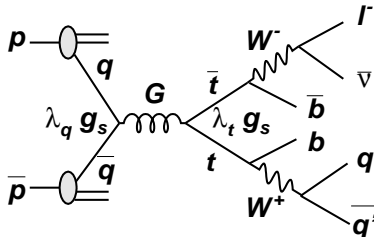


Figure 1: A Feynman diagram showing $t\bar{t}$ production via a massive gluon in the “lepton+jets” decay channel.

2. Selection of candidate events

The search is based on data collected with the CDF II detector between March 2002 and May 2007 at the Fermilab Tevatron $p\bar{p}$ collider, corresponding to an integrated luminosity of about 1.9 fb^{-1} . The CDF II detector is a general purpose detector which is azimuthally and forward-backward symmetric. The detector consists of a charged particle tracking system composed of silicon microstrip detectors and a gas drift chamber inside a 1.4 T magnetic field, surrounded by electromagnetic and hadronic calorimeters and enclosed by muon detectors. The details of the detector are described elsewhere [13].

The cross section for standard model $t\bar{t}$ production in $p\bar{p}$ collisions at $\sqrt{s} = 1.96 \text{ TeV}$ is dominated by $q\bar{q}$ annihilation ($\sim 85\%$). The remaining $\sim 15\%$ is attributed to gluon-gluon fusion [14]. Standard model top quarks decay almost exclusively to Wb . The search presented here focuses on the $t\bar{t}$ event topology wherein one W boson decays hadronically while the other decays to an electron or muon and its corresponding neutrino. Both b quarks and the two decay quarks of the second W boson appear as jets in the detector. Accordingly, $t\bar{t}$ candidates in this “lepton + jets” channel are characterized by a single lepton, missing transverse energy \cancel{E}_T [15], due to the undetected neutrino, and four jets.

We use lepton triggers that require an electron or muon with $p_T > 18 \text{ GeV}/c$. Events included in our analysis must first contain an isolated electron (muon) with $E_T > 20 \text{ GeV}$ ($p_T > 20 \text{ GeV}/c$) in the central detector region with $|\eta| < 1.0$. Electron and muon identification methods are described in Ref. [16]. We remove events which have multiple leptons, cosmic ray muons, electrons from photon-conversion, or tracks, such that its momenta added to the primary lepton momenta gives an invariant mass equal to the Z mass. The position of the primary vertex (along the beam) is required to be within 60 cm of the center of the nominal beam intersection and consistent with the reconstructed z position of the high- p_T lepton. Events must also feature at least 20 GeV of \cancel{E}_T attributable to the presence of a high- p_T neutrino, as well as exactly four jets with $|\eta| < 2.0$ and $E_T > 20 \text{ GeV}$ (jet E_T corrections are described in Ref. [17]). Jets are clustered with a cone-based algorithm, with a cone size

Table 1: Background composition to the $q\bar{q} \rightarrow t\bar{t}$ process and the expected numbers of events. Systematic uncertainties coming from the background estimation method are listed. Electroweak includes single top quark, diboson production, and Z bosons + jets productions. A luminosity of 1.9 fb^{-1} is assumed.

Source	Expected number of events
Electroweak	9.9 ± 0.5
W + bottom	16.5 ± 6.7
W + charm	12.9 ± 5.2
Mistags	16.7 ± 3.6
non- W	13.6 ± 11.7
SM $gg \rightarrow t\bar{t}$	48.2 ± 15.6
Total Background ($n_b^{\text{exp}} \pm \sigma_b^{\text{exp}}$)	117.8 ± 19.8
SM $q\bar{q} \rightarrow t\bar{t}$ ($\sigma = 5.6 \text{ pb}$)	211.7 ± 29.3
Data	371

$\Delta R \equiv \sqrt{\Delta\phi^2 + \Delta\eta^2} = 0.4$. We reduce non- $t\bar{t}$ backgrounds by requiring at least one jet identified by the displaced secondary vertex “ b -tagging” algorithm [13] as being consistent with the decay of a long-lived b hadron.

3. Background

The background to the $t\bar{t}$ signal is mostly from W +jets events with a falsely-reconstructed secondary vertex (Mistags) or from W +jets events where one or more jets are due to heavy-flavor quarks. Smaller contributions are from QCD multi-jet production, in which either the W signature is faked when jets contain semi-leptonic b -hadron decays or when jets are mis-reconstructed and appear as electrons and missing E_T , single top quark production, diboson (WW , WZ , ZZ) production, and Z bosons produced in association with multiple jets. The methods used to estimate the backgrounds are detailed in Ref. [13]. The $gg \rightarrow t\bar{t}$ process is taken as a background for this search, which is estimated by assuming 0.16 ± 0.05 gluon fusion fraction from Ref. [14]. The estimated backgrounds in the sample are summarized in Table 1. The diboson and $gg \rightarrow t\bar{t}$ background processes are modeled with PYTHIA [18], W +jets and Z +jets processes with ALPGEN [19], and QCD with data.

4. $t\bar{t}$ invariant mass reconstruction

We search for a massive gluon by examining the $t\bar{t}$ invariant mass ($\sqrt{\hat{s}_{t\bar{t}}}$) spectrum of the selected events. Our analysis procedure consists of two steps. (A) We first reconstruct the parton level momentum set of $t\bar{t} = (bl^+\nu)(\bar{b}l^-\bar{\nu})$, event-by-event, with the Dynamical Likelihood Method (DLM) [20, 21]. The

likelihood in DLM is defined by the differential cross section per unit phase space volume, multiplied by a posterior transfer function (TF), which is a probability density function from the observed to the parton kinematic quantities. For a given event, different parton kinematics set are inferred with TF. We assume in this paper the TF is independent of the production matrix for $t\bar{t}$, hence in the reconstruction, we remove the $t\bar{t}$ production matrix from the likelihood. For each event the reconstructed $\sqrt{\hat{s}_{t\bar{t}}}$ is averaged over inferred parton paths, and denoted by $\sqrt{\hat{s}_r}$. We denote the true $\sqrt{\hat{s}_{t\bar{t}}}$ at the parton level by $\sqrt{\hat{s}_p}$.

(B) We interpret $\sqrt{\hat{s}_r}$ as an observed quantity and apply a standard unbinned likelihood technique to reproduce the $\sqrt{\hat{s}_r}$ distribution using Monte Carlo (MC) events, which consist of signal and relevant background processes.

The $\sqrt{\hat{s}_r}$ distribution for the signal $g + G$ process is expressed relative to $[d\sigma/d\sqrt{\hat{s}_p}]_{SM:q\bar{q}\rightarrow t\bar{t}}^*$, the SM cross section after the event selection cuts (expressed by $*$) by

$$p_s[\sqrt{\hat{s}_r}; \boldsymbol{\alpha}] \equiv N(\boldsymbol{\alpha}) \int \left[\frac{d\sigma}{d\sqrt{\hat{s}_p}} \right]_{SM:q\bar{q}\rightarrow t\bar{t}}^* R(\sqrt{\hat{s}_p}; \boldsymbol{\alpha}) f(\sqrt{\hat{s}_r} - \sqrt{\hat{s}_p}; \sqrt{\hat{s}_p}) d\sqrt{\hat{s}_p}, \quad (3)$$

where $\boldsymbol{\alpha} \equiv (\lambda, M, \Gamma)$ is a set of massive gluon parameters, and $N(\boldsymbol{\alpha})$ is the normalization factor. The ratio of $g + G$ to SM $t\bar{t}$ production cross sections is

$$R(\sqrt{\hat{s}_p}; \boldsymbol{\alpha}) = 1 + 2\lambda \frac{\hat{s}_p(\hat{s}_p - M^2)}{(\hat{s}_p - M^2)^2 + M^2\Gamma^2} + \lambda^2 \frac{\hat{s}_p^2}{(\hat{s}_p - M^2)^2 + M^2\Gamma^2}. \quad (4)$$

In this ratio, PDF effects, top propagators, decay matrix elements and the final state densities for $g + G$ and SM processes cancel out, making it possible to generate (or derive) $g + G$ events with specified $\boldsymbol{\alpha}$ from standard model $t\bar{t}$ MC events. The resolution function f translates $\sqrt{\hat{s}_p}$ to $\sqrt{\hat{s}_r}$. It is obtained from the scatter plot of $\sqrt{\hat{s}_r} - \sqrt{\hat{s}_p}$ vs. $\sqrt{\hat{s}_p}$ using the PYTHIA SM $q\bar{q} \rightarrow t\bar{t}$ MC sample, as shown in Fig. 2. The peak and half maximum points of $\sqrt{\hat{s}_r} - \sqrt{\hat{s}_p}$ are typically $-0.2^{+15.7}_{-13.7}$, $-0.9^{+31.0}_{-40.7}$, and $-3.5^{+39.6}_{-68.7}$ GeV/ c^2 at $\sqrt{s_p} = 400, 600,$ and 800 GeV/ c^2 , respectively.

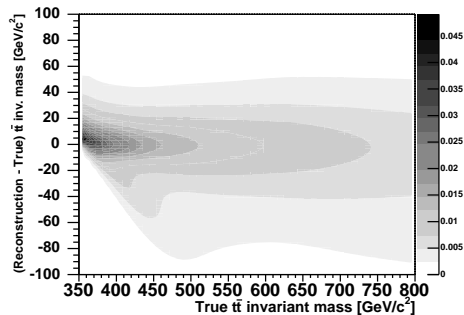


Figure 2: Resolution function $f(y; x)$, where $x = \sqrt{\hat{s}_p}$ and $y = \sqrt{\hat{s}_r} - \sqrt{\hat{s}_p}$.

Figure 3 shows an example of $p_s[\sqrt{\hat{s}_r}; \alpha]$. The first(second) peak is due to $g(G)$. At the parton level, the G peak(dip) is above(below) M for positive(negative) λ , while at the reconstructed $\sqrt{\hat{s}_r}$ distribution the peak(dip) is shifted due to the resolution function. The PYTHIA MC with $M_t = 175 \text{ GeV}/c^2$ is used to estimate $[d\sigma/d\sqrt{\hat{s}_p}]_{SM:q\bar{q}\rightarrow t\bar{t}}$.

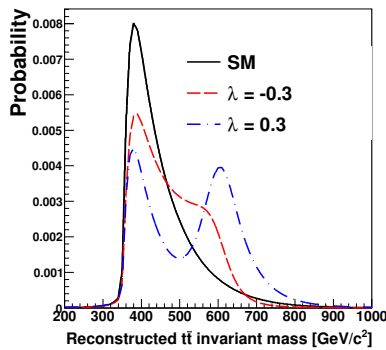


Figure 3: Signal probability density function $p_s[\sqrt{\hat{s}_r}; \alpha]$ with $M = 600 \text{ GeV}/c^2$, $\Gamma/M = 0.10$, and $\lambda = \pm 0.3$.

5. Extraction of coupling strength

If M and Γ/M are given, the $\sqrt{\hat{s}_r}$ distribution of the data is a function of λ and the numbers of the signal and background events, n_s and n_b . By applying a three parameter unbinned likelihood method for (λ, n_s, n_b) , the likelihood function L for the distribution is

$$L\left(\lambda, n_s, n_b \middle| M, \frac{\Gamma}{M}\right) \equiv G(n_b; n_b^{\text{exp}}, \sigma_b^{\text{exp}}) P(N; n) \prod_{i=1}^N \frac{n_s p_s(\sqrt{\hat{s}_r}(i); \alpha) + n_b p_b(\sqrt{\hat{s}_r}(i))}{n}. \quad (5)$$

Function $G(n_b; n_b^{\text{exp}}, \sigma_b^{\text{exp}})$ constrains the total background normalization with Gaussian probability around the central value n_b^{exp} and its uncertainty σ_b^{exp} as given in Table 1. $P(N; n)$ is the Poisson probability for observing N events where $n = n_s + n_b$ are expected. $p_s(\sqrt{\hat{s}_r}(i); \alpha)$ and $p_b(\sqrt{\hat{s}_r}(i))$ are probability densities that the i -th event is due to signal or background, respectively. We calculate the likelihood as a function of λ for a number of values of $(M, \Gamma/M)$, where the value of M ranges from 400 to 800 GeV/c^2 at 50 GeV/c^2 intervals. Γ/M is considered at values of 0.05, 0.1, 0.2, 0.3, 0.4 and 0.5.

The analysis method is tested with pseudo-experiments (PE's), where the background events are generated according to Table 1, and the total number of events is normalized to the 371 observed number of candidate events. An example of the analysis of a single pseudo-experiment is shown in Fig. 4. Points represent the observed $\sqrt{\hat{s}}$ distribution for a simulated signal sample with $\Gamma/M = 0.1$, $M = 600 \text{ GeV}/c^2$ and $\lambda = 0.1$. λ is estimated by maximizing the likelihood L , given the observed $\sqrt{\hat{s}_r}$ spectrum. The 95% C.L. lower/upper two-sided limit on λ at the given mass and width is found by taking $-2 \ln(L/L_{max}) = 3.84$. We measure our expected sensitivity using a large number of null signal PE's.

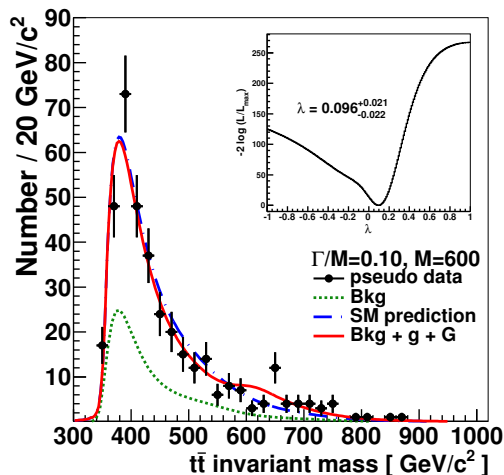


Figure 4: An example of a likelihood fit to $\sqrt{\hat{s}_r}$ spectrum for 1.9 fb^{-1} MC events (points), which includes the massive gluon with a $\Gamma/M = 0.1$, $M = 600 \text{ GeV}/c^2$, and $\lambda = 0.1$. The solid line is the best fit to a superposition of $g + G$ signal and the expected background (dash line) and SM prediction (dot-dash line). The likelihood fit is performed assuming $\Gamma/M = 0.1$ and $M = 600 \text{ GeV}/c^2$. The inset shows the $-2 \ln L$ as a function of λ .

We have studied contributions to the total uncertainty arising from systematic effects. Variation of the $t\bar{t}$ invariant mass distribution affects the estimation of the coupling strength, λ . The jet energy scale and top-quark mass are varied simultaneously (within their uncertainties) to properly account for their correlation. The uncertainties of the parton distribution functions (PDF) are estimated by comparing PE's where different PDF sets (CTEQ5L[22] vs MRST72[23]) are used; additionally, Λ_{QCD} and the CTEQ6M[22] PDF eigenvectors are varied. The systematic effect due to choice of MC generator is estimated by comparing PE's using events generated by PYTHIA and HERWIG [24]. The scale of next-to-leading-order systematic effects is estimated by using events generated with MC@NLO[25]. Systematic uncertainties in modeling initial- and final-state gluon radiation are estimated using PYTHIA, where the range of QCD parameters are varied in accordance with CDF studies of Drell-Yan data [26]. The uncertainty in the MC modeling of the multiple interaction and the b -tagging efficiency as a function of jet p_T are evaluated. All systematic uncertainties are evaluated at the full range of coupling strengths, gluon masses and decay widths considered, and are incorporated in the likelihood function.

6. Results

The $t\bar{t}$ invariant mass distribution observed in data is shown in Fig. 5. The best fit of λ is consistent with the SM prediction, including a fluctuation of $\sim 1.7\sigma$ within the explored parameter range. We search for massive gluon with mass in the range $[400,800]$ GeV/ c^2 , though events with gluon masses beyond this region are included in the analysis. The 95% C.L. limits on the coupling strength λ at $\Gamma/M = 0.1$ and $\Gamma/M = 0.5$ are shown in Fig. 6. A less stringent limit above 650 GeV/ c^2 is due to 4 events on the high mass tail. The SM predicts 1.4 events above 850 GeV/ c^2 , 4 events observed correspond to a Poisson probability of 5.4 %. The limits at 95% C.L. for several values of M and Γ/M are listed in Table 2. The limits become weaker with higher M and wider Γ/M .

In conclusion, we perform an exploratory search for a color-octet vector particle in general with minimal model dependence. No significant indication of the existence of massive gluon with $|\lambda| > 0.5$ is observed in our search region of $400 \text{ GeV}/c^2 < M < 800 \text{ GeV}/c^2$ and $0.05 < \Gamma/M < 0.5$.

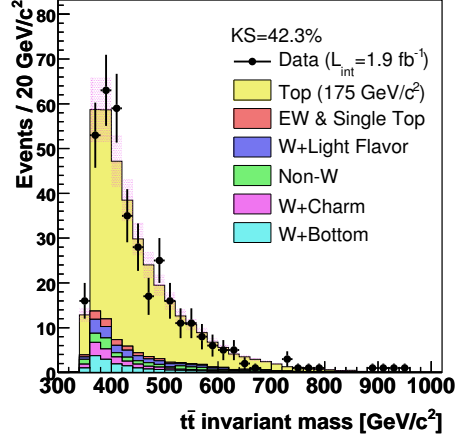


Figure 5: The $t\bar{t}$ invariant mass distribution. The points represent the observed distribution; the histogram represents the SM prediction normalized to the observed data. The pink bands represent the uncertainty on the background estimations.

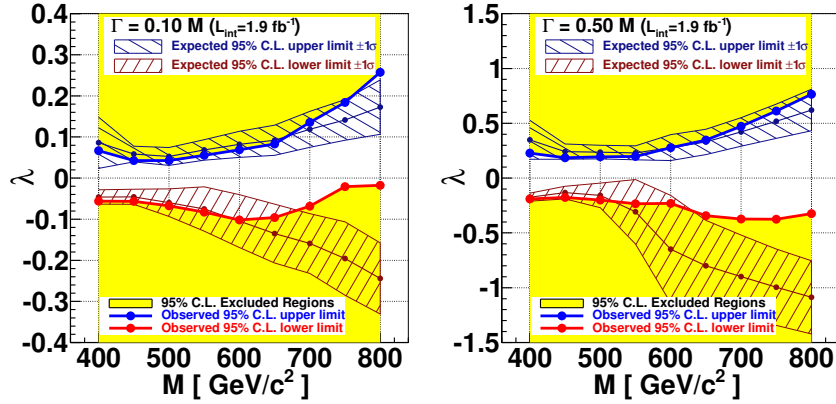


Figure 6: Excluded regions of λ in the λ - M plane (yellow), for $\Gamma/M = 0.1$ (left) and $\Gamma/M = 0.5$ (right). The expected limit is defined as median 95% value and $\pm 1\sigma$ is defined with regard to the median for the set of null signal PE's.

Table 2: Expected and observed 95% C.L. lower/upper limits on λ . Expected limits are in parentheses.

	$F/M = 0.05$	$F/M = 0.10$	$F/M = 0.20$	$F/M = 0.30$	$F/M = 0.40$	$F/M = 0.50$
M=400	(-0.036 / 0.042)	(-0.046 / 0.086)	(-0.074 / 0.156)	(-0.11 / 0.26)	(-0.15 / 0.30)	(-0.17 / 0.35)
	-0.043 / 0.040	-0.056 / 0.067	-0.089 / 0.11	-0.12 / 0.18	-0.16 / 0.20	-0.19 / 0.23
M=450	(-0.038 / 0.040)	(-0.046 / 0.058)	(-0.065 / 0.087)	(-0.087 / 0.13)	(-0.12 / 0.19)	(-0.13 / 0.24)
	-0.045 / 0.027	-0.057 / 0.042	-0.086 / 0.06	-0.12 / 0.09	-0.15 / 0.14	-0.18 / 0.19
M=500	(-0.051 / 0.038)	(-0.060 / 0.053)	(-0.083 / 0.087)	(-0.12 / 0.13)	(-0.13 / 0.18)	(-0.16 / 0.24)
	-0.059 / 0.034	-0.067 / 0.043	-0.10 / 0.06	-0.14 / 0.10	-0.17 / 0.14	-0.20 / 0.19
M=550	(-0.058 / 0.049)	(-0.075 / 0.069)	(-0.13 / 0.10)	(-0.15 / 0.15)	(-0.20 / 0.20)	(-0.31 / 0.23)
	-0.064 / 0.039	-0.083 / 0.055	-0.12 / 0.08	-0.16 / 0.13	-0.19 / 0.18	-0.23 / 0.20
M=600	(-0.074 / 0.058)	(-0.10 / 0.082)	(-0.19 / 0.12)	(-0.21 / 0.18)	(-0.35 / 0.22)	(-0.65 / 0.28)
	-0.073 / 0.048	-0.10 / 0.069	-0.16 / 0.10	-0.15 / 0.16	-0.22 / 0.20	-0.23 / 0.28
M=650	(-0.098 / 0.077)	(-0.14 / 0.092)	(-0.24 / 0.15)	(-0.36 / 0.20)	(-0.58 / 0.27)	(-0.80 / 0.33)
	-0.081 / 0.069	-0.096 / 0.083	-0.13 / 0.15	-0.16 / 0.20	-0.26 / 0.29	-0.34 / 0.35
M=700	(-0.11 / 0.082)	(-0.16 / 0.12)	(-0.27 / 0.17)	(-0.44 / 0.25)	(-0.68 / 0.32)	(-0.90 / 0.42)
	-0.070 / 0.091	-0.068 / 0.14	-0.091 / 0.19	-0.13 / 0.29	-0.31 / 0.37	-0.37 / 0.47
M=750	(-0.14 / 0.11)	(-0.20 / 0.14)	(-0.33 / 0.21)	(-0.50 / 0.31)	(-0.71 / 0.39)	(-1.00 / 0.52)
	-0.020 / 0.13	-0.021 / 0.18	-0.033 / 0.26	-0.03 / 0.38	-0.06 / 0.47	-0.37 / 0.61
M=800	(-0.16 / 0.12)	(-0.24 / 0.17)	(-0.39 / 0.27)	(-0.59 / 0.37)	(-0.80 / 0.49)	(-1.09 / 0.62)
	-0.011 / 0.18	-0.017 / 0.26	0.017 / 0.37	-0.04 / 0.50	-0.01 / 0.63	-0.33 / 0.76

Acknowledgements

We thank the Fermilab staff and the technical staffs of the participating institutions for their vital contributions. This work was supported by the U.S. Department of Energy and National Science Foundation; the Italian Istituto Nazionale di Fisica Nucleare; the Ministry of Education, Culture, Sports, Science and Technology of Japan; the Natural Sciences and Engineering Research Council of Canada; the National Science Council of the Republic of China; the Swiss National Science Foundation; the A.P. Sloan Foundation; the Bundesministerium für Bildung und Forschung, Germany; the World Class University Program, the National Research Foundation of Korea; the Science and Technology Facilities Council and the Royal Society, UK; the Institut National de Physique Nucleaire et Physique des Particules/CNRS; the Russian Foundation for Basic Research; the Ministerio de Ciencia e Innovación, and Programa Consolider-Ingenio 2010, Spain; the Slovak R&D Agency; and the Academy of Finland.

References

- [1] C.T. Hill and S.J. Parke, Phys. Rev. D 49 (1994) 4454.
- [2] C.T. Hill, Phys. Lett. B 345 (1995) 483.
- [3] K. J. F. Gaemers and F. Hoogeveen, Phys. Lett. B 146 (1984) 347.
- [4] D. Dicus, A. Stange and S. Willenbrock, Phys. Lett. B 333 (1994) 126.
- [5] A. Leike, Phys. Rept. 317 (1999) 143.
- [6] B. Lillie, L. Randall, L.-T. Wang, J. High Energy Phys. 09 (2007) 074.
- [7] T. G. Rizzo, Phys. Rev. D 61 (2000) 055005.

- [8] T. Affolder *et al.* (CDF Collaboration), Phys. Rev. Lett. 85 (2000) 2062.
- [9] V. M. Abazov *et al.* (D0 Collaboration), Phys. Rev. Lett. 92 (2004) 221801.
- [10] T. Aaltonen *et al.* (CDF Collaboration), Phys. Rev. Lett. 100 (2008) 231801.
- [11] T. Aaltonen *et al.* (CDF Collaboration), Phys. Rev. D 77 (2008) 051102.
- [12] T. M. Abazov *et al.* (D0 Collaboration), Phys. Lett. B 668 (2008) 98.
- [13] D. Acosta *et al.* (CDF Collaboration), Phys. Rev. D 71 (2005) 032001.
- [14] M. Cacciari *et al.*, J. High Energy Phys. 0404 (2004) 68.
- [15] We use a coordinate system defined about the proton beam direction, which is taken as the z axis; the x axis lies in the horizontal plane. Then θ is the usual polar angle and ϕ is the azimuthal angle. We define the pseudorapidity η of a particle's three-momentum as $\eta \equiv -\ln(\tan \frac{\theta}{2})$. The transverse energy and momentum are defined as $E_T = E \sin \theta$ and $p_T = p \sin \theta$ where E is the energy measured by the calorimeter and p is the momentum measured in the tracking system. The missing transverse energy is defined as $\cancel{E}_T = |-\sum_i E_T^i \vec{n}_i|$ where \vec{n}_i is a unit vector in the transverse plane that points from the event vertex to the azimuth of the i^{th} calorimeter tower.
- [16] A. Abulencia *et al.* (CDF Collaboration), J. Phys. G: Nucl. Part. Phys. 34 (2007) 2457.
- [17] A. Bhatti *et al.*, Nucl. Instrum. Methods, A 566 (2006) 375.
- [18] T. Sjöstrand *et al.*, Computer Physics Commun. 135 (2001) 238.
- [19] M.L. Mangano *et al.*, J. High Energy Phys. 0307 (2003) 001.
- [20] K. Kondo, J. Phys. Soc. Jpn. 57 (1988) 4126; K. Kondo, hep-ex/0508035.
- [21] A. Abulencia *et al.* (CDF Collaboration), Phys. Rev. D 73 (2006) 092002.
- [22] J. Pumplin *et al.*, J. High Energy Phys. 0207 (2002) 012.
- [23] A. D. Martin *et al.*, Phys. Lett. B 356 (1995) 89.
- [24] G. Marchesini and B.R. Webber, Nucl. Phys. B 310 (1988) 461; G. Marchesini *et al.*, Comput. Phys. Commun. 67 (1992) 465.
- [25] S. Frixione *et al.*, J. High Energy Phys. 06 (2002) 029.
- [26] A. Abulencia *et al.*, Phys. Rev. D 73 (2006) 032003.